J|A|C|S
COMMUNICATIONS

Published on Web 04/12/2006

Chemical Routes to Nanocrystalline Thermoelectrically Relevant $AgPb_mSbTe_{m+2}$ Materials

Abhijeet J. Karkamkar and Mercouri G. Kanatzidis*

Department of Chemistry, Michigan State University, East Lansing, Michigan 48823

Received January 17, 2006; E-mail: kanatzid@cem.msu.edu

Materials with compositions $AgSbTe_2$ and $AgPb_mSbTe_{m+2}$ have been shown to have promising thermoelectric (TE) properties.[1] Recently, we described the chalcogenide compounds, $AgPb_m$-$SbTe_{m+2}$, or LAST-*m* materials (LAST for Lead Antimony Silver Tellurium), several members of which can exhibit large ZT values from ~1.2 to ~1.7 (LAST-10 and -18) at 700 K.[2] High resolution transmission electron microscopy images (HRTEM) of these samples revealed endotaxially dispersed nanocrystals (i.e. regions 2−5 nm in size that are $AgPb_mSbTe_{m+2}$ where $m \approx 1-4$.[3] The nanocrystals are reminiscent of those found in the molecular beam epitaxy-grown, high-performance TE PbTe/PbSe thin films which also exhibit high ZT values (2.5 at 500 K).[4] The nanocrystals are believed to impact the thermoelectric properties at least in part by causing enhanced phonon scattering leading to very low thermal conductivity. This is amply supported by theoretical investigations which also suggest enhancements in power factor.[5] It would therefore be interesting to develop an approach of fabricating nano-phased LAST materials using benchtop inexpensive routes to conduct further studies and to investigate the link to enhanced TE performance. Here we report the synthesis of nanoparticles with compositions $AgSbTe_2$, $AgPbSbTe_3$, and $AgPb_2SbTe_4$ using reverse micellar synthesis[6,7] coupled with a sodium borohydride reduction. In this route all metal ions, Ag^+, Pb^{2+}, Sb^{3+} including Te^{4+} (in Na_2TeO_3), are probably simultaneously reduced to the elemental nanoparticles which combine to form the quaternary phases.

Nanoparticles of binary chalcogenides (e.g., CdSe, PbTe) are very well studied and relatively easy to synthesize with a high degree of control using a high-boiling solvent such as trioctyl-phosphine oxide (TOPO) with elemental chalcogenide and a appropriate metal salt as a precursor.[8−10] However, ternary or quaternary systems tend to be more challenging as they can face problems of phase separation and limitations of solubility of one or more of the precursors in a common solvent. Notable successes, however, in the synthesis of non-oxidic ternary nanoparticles have been achieved.[11] We explored a variety of approaches including high-boiling TOPO, reverse micelles, and capping agents in water. The use of TOPO as a capping agent with elemental Te for the synthesis of $AgSbTe_2$ as a precursor resulted in compounds with low crystallinity and a mixture of Sb_2Te_3, Ag_2Te, and Te. Another problem was the parasitic reduction of silver salts at higher temperatures, yielding metallic silver precipitates in the reaction mixture. The TOPO approach suffered from a lack of proper precursors of Sb^{3+} ions with suitable solubility and was not pursued. We were successful with the capping agent[12] and reverse micellar[13] approaches. The use of hexadecyl-amine as a capping agent yielded good-quality nanoparticles with high degree and crystallinity using $NaBH_4$ reduction but often resulted in excessive aggregation. Although the fundamental particle size was fairly small, 5−15 nm, the $AgSbTe_2$ particles tended to agglomerate and form discontinuous networks. Nanoparticles exhibiting no aggregation were obtained only with a reverse micelle-based approach[14,15] and a borohydride-based co-reduction, and this method was adopted for further work.

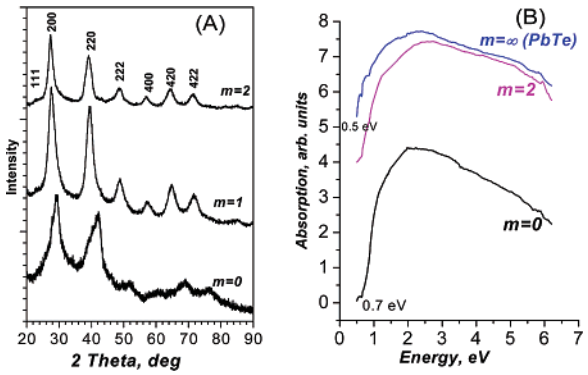

Figure 1. (A) XRD patterns (Cu Kα rad) of nanoparticles of $AgSbTe_2$ ($m = 0$), $AgPbSbTe_3$ ($m = 1$), and $AgPb_2SbTe_4$ ($m = 2$). (B) Solid-state optical band gap measurement for $m = 0$, 2 and for comparison PbTe ($m = \infty$). Diffuse reflectance data converted to absorption using the Kubleka−Munk function (SI). The spectra are offset along the *y*-axis.

Table 1. Elemental Composition, Lattice Constant (Å), Average Particle Size, and Energy Band Gap (E_g) for $AgPb_mSbTe_{m+2}$ Nanoparticles

sample	composition (esd ±4–5%)[a]	cell parameter (Å)	particle size[b] (nm)	E_g (eV)[c]
$m = 0$	$Ag_{1.07}SbTe_{2.08}$	6.10(1)	4.3	0.7(1)
$m = 1$	$Ag_{0.95}PbSb_{1.07}Te_{2.67}$	6.42(1)	4.6	0.6(1)
$m = 2$	$Ag_{1.15}Pb_2Sb_{0.86}Te_{4.10}$	6.45(1)	5.2	0.6(1)
$m = \infty$	$Pb_{1.00}Te_{0.99}$	6.55(1)	5.0	0.5(1)

[a] SEM-EDS analysis. [b] Average size from XRD data (error ±10%). [c] The optical spectra were measured in the diffuse reflectance mode on a Shimadzu UV−vis−NIR spectrophotometer (UV3101 PC).

Namely nanocrystals of $AgPb_mSbTe_{m+2}$ ($m = 0-2$) were synthesized in a reversed micellar solution of sodium dodecyl sulfate (SDS) under ambient conditions. SDS reverse micelles were prepared using octane, 1-butanol, and water as solvents. The preferred precursors were lead nitrate, potassium antimony tartrate, and silver nitrate. Potassium telluride (K_2Te) or sodium tellurite (Na_2TeO_3) were used as the tellurium sources. Nanocrystals of $AgSbTe_2$ required K_2Te as the precursor,[16] whereas $AgPbSbTe_3$ and $AgPb_2SbTe_4$ were prepared with Na_2TeO_3 followed by reduction with $NaBH_4$.

The nanoparticles obtained from the synthesis had approximate spherical geometry and were crystalline with size dispersity ranging between 3 and 15 nm. The powder XRD patterns show broadening of Bragg peaks with a characteristic cubic NaCl-type structure and $Fm\bar{3}m$ space group, Figure 1. The lattice parameters lie between those of $AgSbTe_2$ and PbTe and vary systematically with *m* (see Table 1) which is evidence for the successful incorporation of $AgSbTe_2$ into the PbTe lattice. They also compare well to those of the bulk LAST materials synthesized with conventional solid-state

10.1021/ja060352r CCC: $33.50

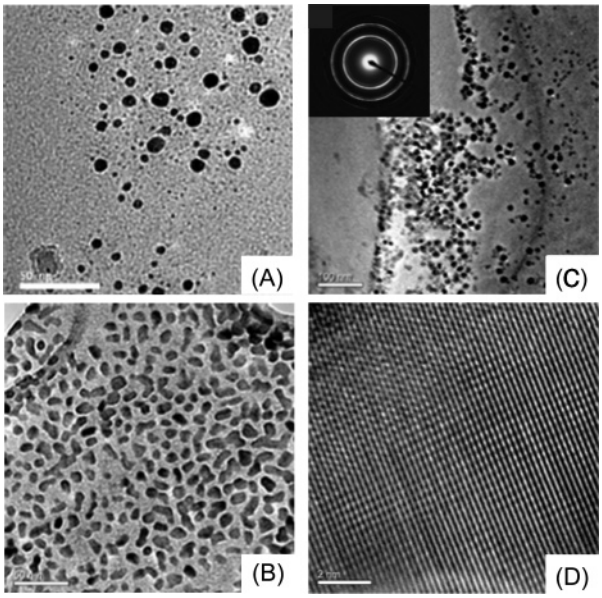

Figure 2. TEM images of nanoparticles: low magnification image of (A) $AgSbTe_2$, (B) $AgPbSbTe_3$, and (C) $AgPb_2SbTe_4$. (Inset) Electron diffraction pattern of a collection of nanoparticles consistent with $Fm\bar{3}m$ lattice. (D) HRTEM image of $AgPb_2SbTe_4$, showing the presence of lattice fringes with ~6.5 Å period. The scale bars in the four images are 50, 50, 100, and 2 nm respectively. EDS analysis on individual nanocrystals indicated the presence of all four elements. High-resolution TEM images were obtained with 200 kV JEOL JEM 2200FS microscope.

synthesis. The average particle sizes estimated from line broadening analysis are in the range of ~4.5−5.2 nm and in agreement with the TEM observations, see Table 1.[17]

The nanoparticles ($m = 0-2$) show well-defined energy band gaps in the range of ~0.6−0.7 eV, Figure 1B and Table 1. These band gaps are significantly wider than the corresponding values of the bulk materials of ~0.3 eV which is consistent with the expected size-dependent blue-shift due to quantization of the energy levels in the nanocrystals.

Figure 2A shows a low-magnification TEM image of $AgSbTe_2$, indicating nanoparticles ranging from 3 to 15 nm, over a large area. Similar particle size distributions were obtained for $AgPb_2SbTe_4$ and $AgSbPbTe_3$, Figure 2B,C. Figure 2D shows a HRTEM image of a single nanocrystal of $AgPb_2SbTe_4$ prepared with the reverse micellar approach. Energy-dispersive X-ray spectroscopy analysis (EDS) on individual nanoparticles indicated the presence of all four elements. The lattice fringes are clearly visible in the image, indicating high atomic order. We did not observe any evidence for amorphous products by TEM. Furthermore, the XRD patterns as well as SEM investigations indicated no evidence for adventitious phases such as Ag, Ag_2Te, Sb_2Te_3, or Te (detection limit ~±5%). Electron diffraction patterns obtained from collections of these nanoparticles indicated only rock-salt $Fm\bar{3}m$ structure type, Figure 2C (inset). EDS analysis of $AgPb_mSbTe_{m+2}$ in a scanning electron microscope showed presence of Ag, Sb and Pb, and Te in atomic ratios summarized in Table 1.

In conclusion, a facile synthesis of nanoparticles of the thermoelectrically relevant $AgPb_mSbTe_{m+2}$ was accomplished for the first time in reverse micelles. The procedure offers several distinct advantages for the synthesis of crystalline nanoparticles of thermoelectric ternary and quaternary lead chalcogenides. The process is convenient, general, and extendable to nanoparticles with higher m values including $m = \infty$ (i.e., PbTe). It is also low cost and environmentally friendly, by employing common water-soluble metal salts. As a result, the synthesis could be scaled to a multigram level in a single reaction. We are currently investigating methods to process these nanomaterials into compact shapes and measure their thermoelectric properties. Additionally, nanoparticles of LAST could show unusual electronic and optical properties that could help in understanding the corresponding bulk materials. This is a challenging task owing to a coating of the organic layer surrounding the nanoparticles. Various techniques, including annealing, extraction of surfactants with suitable solvents, followed by cold or hot pressing, for conductivity and thermopower measurements are in progress.

Acknowledgment. Financial support from the Office of Naval Research (N00014-02-1-0867) is gratefully acknowledged.

Supporting Information Available: Details of synthetic protocols, SEM images, and EDS analysis. This material is available free of charge via the Internet at http://pubs.acs.org.

References

(1) (a) Hockings, E. F. *Phys. Chem. Solids* **1959**, *10*, 341−342. (b) Irie, T.; Takahama, T.; Ono, T. *Jpn. J. Appl. Phys.* **1963**, *2*, 72−82. (c) Maier, R. G. *Z. Metallkunde* **1963**, *54*, 311−312.
(2) Hsu, K. F.; Loo, S.; Guo, F.; Chen, W.; Dyck, J. S.; Uher, C.; Hogan, T.; Polychroniadis, E. K.; Kanatzidis, M. G. *Science* **2004**, *303*, 818−821.
(3) Quarez, E.; Hsu, K.-F.; Pcionek, R.; Frangis, N.; Polychroniadis, E. K.; Kanatzidis, M. G. *J. Am. Chem. Soc.* **2005**, *127*, 9177−9190.
(4) Harman, T. C.; Taylor, P. J.; Walsh, M. P.; LaForge, B. E. *Science* **2002**, *297*, 2229−2232.
(5) Khitun, A.; Wang, K. L.; Chen, G. *Nanotechnology* **2002**, *11*, 327−331.
(6) Zhou, Z. H.; Wang, J.; Liu, X.; Chan, H. S. O. *J. Mater. Chem.* **2001**, *11*, 1704−1709.
(7) Fried, T.; Shemer, G.; Markovich, G. *Adv. Mater.* **2001**, *13*, 1158−1161.
(8) (a) Alivisatos, A. P. *Science* **1996**, *271*, 933−937. (b) Jacobs, K.; Zaziski, D.; Scher, E. C.; Herhold, A. B.; P. Alivisatos, A. *Science* **2001**, *293*, 1803−1806.
(9) (a) Chen, F.; Stokes, K. L.; Zhou, W.; Fang, J.; Murray, C. B. *Mater. Res. Soc. Symp. Proc.* **2002**, *691*, 359−364. (b) Lu, W. G.; Fang, J. Y.; Stokes, K. L.; Lin, J. *J. Am. Chem. Soc.* **2004**, *126*, 11798−11799.
(10) (a) Du, H.; Chen, C.; Krishnan, R.; Krauss, T. D.; Harbold, J. M.; Wise, F. W.; Thomas, M. G.; Silcox, J. *Nano Lett.* **2002**, *2*, 1321−1324. (b) Murray, C. B.; Kagan, C. R.; Bawendi, M. G. *Science* **1995**, *270*, 1335−1338.
(11) (a) Gurin, V. S. *Colloid Surf. Physicochem. Eng. Asp.* **1998**, *142*, 35−40. (b) Leonard, B. M.; Bhuvanesh, N. S. P.; Schaak, R. E. *J. Am. Chem. Soc.* **2005**, *127*, 7326−7327.
(12) Aslam, M.; Fu, L.; Su, M.; Vijayamohanan, K.; Dravid, V. P. *J. Mater. Chem.* **2004**, *14*, 1795−1797.
(13) Lee, Y.; Lee, J.; Bae, C. J.; Park, J.-G.; Noh, H.-J.; Park, J.-H.; Hyeon, T. *Adv. Funct. Mater.* **2005**, *15*, 503−509.
(14) Agnoli, F.; Zhou, W. L.; O'Connor, C. J. *Adv. Mater.* **2001**, *13*, 1697−1699.
(15) Hong, C.-Y.; Jang, I. J.; Horng, H. E.; Hsu, C. J.; Yao, Y. D.; Yang, H. C. *J. Appl. Phys.* **1997**, *81*, 4275−4277.
(16) Reverse micellar solutions of sodium dodecyl sulfate (SDS) were prepared in a sealed vial as described elsewhere.[14,15] An amount of 3 g of SDS was mixed with 11 g of octane and 2.5 g of 1-butanol to form a milky solution. An amount of 1.5 gm of water was then added to the milky solution to form a clear solution upon stirring. The solution was allowed to stir for 1 h and then allowed to stand for 2 h. No turbidity or settling was observed over this period. Five such reverse micellar solutions were prepared, and to each one $AgNO_3$, potassium antimony tartrate, $Pb(NO_3)_2$, Na_2TeO_3/K_2Te, and $NaBH_4$ salts were added, respectively. $AgNO_3$ solutions were kept in a dark vial to prevent reduction to metallic Ag. The molar quantities of all the emulsions were in the range 0.1−0.6 and are summarized in the Supporting Information. The emulsions/solutions of Ag, Sb, and Pb were mixed and allowed to stir for 1 h. The emulsion containing the Te precursor (K_2Te for $m = 0$ and Na_2TeO_3 for $m = 1$ and $m = 2$) was then added to the mixture to form a translucent emulsion. Stirring continued for 2−3 h, and to it the microemulsion containing $NaBH_4$ was then added at once. The color changed instantaneously from translucent milky to black, and the reaction continued for 5−6 h to ensure complete reduction. The reaction mixture was then allowed to stand until the octane evaporated, leaving a white surfactant mass containing black particles. The excess surfactant was washed off with ethanol to yield the black particles.
(17) Klug, H. P.; Alexander, L. E. *X-ray Diffraction Procedures for Polycrystalline and Amorphous Materials*; Wiley: New York, 1954.

JA060352R